

Iranian Journal of Electrical and Electronic Engineering

Journal Homepage: ijeee.iust.ac.ir



An Optimized Magnetic Structure to Enhance Misalignment Tolerance in Wireless Power Transfer Systems for Electric Vehicle Charging

Mohammad Negintaji*, Aghil Ghaheri*(C.A) and Ebrahim Afjei*

Abstract: In the rapidly advancing domain of wireless power transfer systems, particularly for electric vehicle charging, the design of the magnetic coupler plays a crucial role in determining both system efficiency and practical implementation. Variations in coupler system designs lead to differences in self-inductance, mutual inductance, and AC resistance, directly impacting the energy transfer efficiency and power delivery capability of the system. This paper proposes a novel coil design for wireless power transfer systems, incorporating Double-DZ (DDZ) and Quadrature (Q) coils to improve lateral and yaw misalignment tolerance. The proposed design integrates the advantageous features of three structures—SDDP, DDQP and TTP—to introduce a novel configuration, DDZ-DDQZ, which enhances system stability and performance. By increasing misalignment tolerance, this method substantially enhances the robustness and real-world feasibility of wireless power transfer for electric vehicle charging.

Keywords: wireless power transfer, magnetic coupler design, Inductive resonant coupling, Finite element analysis.

1 Introduction

THE rise of electric vehicles (EVs) has marked a **1** transformative shift toward sustainable transportation, underscoring the demand for advanced solutions to overcome the constraints of existing battery technologies [1]. A major obstacle to the widespread adoption of EVs is the inefficiency and lack of convenience inherent in traditional technologies. To address these challenges, wireless power transfer (WPT) systems are progressively being standardized to achieve seamless interoperability.

The design of the magnetic coupler plays a crucial role in determining the efficiency and feasibility of the system. Variations in coil geometry, including different shapes, turn counts, turn spacing, as well as coil diameter and material, significantly impact both self-inductance and mutual inductance, ultimately

influencing the power transfer capability and efficiency of the wireless charging system [2]. Extensive research has been conducted on coil structure design, encompassing various coil geometries, materials, and related parameters. A DD coil coupling mechanism is proposed and optimized to enhance mutual inductance in metallic environments, whereas refinements in ferrite core design within the coil aim to improve system output power and efficiency [3]. Advanced configurations, such as crossed and layered DD coils, are investigated to increase efficiency and address challenges related to coil misalignment and variations in mutual inductance [4], [5]. Additionally, overlapped DD coil arrays are implemented alongside a control strategy that dynamically regulates transmitter currents to optimize energy transfer efficiency [6]. The design and operational characteristics of DD pad structures in WPT systems for electric vehicles are analyzed to improve the magnetic coupling coefficient [7]. Furthermore, the performance of LDD coils is evaluated in comparison to conventional DD coils, with a particular emphasis on inductance characteristics and the impact of different shielding materials, such as ferrite and aluminum [8].

1

Iranian Journal of Electrical & Electronic Engineering, 2026. Paper first received 15 Mar. 2025 and accepted 08 Jul. 2025.

E-mails: <u>m_negintaji@sbu.ac.ir</u>,

^{*} The author is with the Department of Electrical Engineering Shahid Beheshti University, Tehran, Iran.

<u>a_ghaheri@sbu.ac.ir</u>, e-afjei@sbu.ac.ir Corresponding Author: Aghil Ghaheri.

Various methods have been proposed for calculating mutual inductance, self-inductance, and winding resistance without relying on finite element analysis (FEA) software [9]. However, these methods demonstrate acceptable accuracy for basic and fundamental systems but are not applicable to complex and advanced structures. Presents a highly accurate and efficient methodology for calculating Litz wire parameters, specifically tailored for seamless integration with FEA software [10]. The structure of this paper is outlined as follows: Section 2 elaborates on the methodology for designing the magnetic structure. Section 3 explores the development and assessment of five conventional topologies for electric vehicle charging systems, accompanied by a comparative performance analysis. Section 4 details the construction of a prototype employed for validating the simulation findings. Section 5 presents the proposed innovative structure along with its corresponding simulation results. Lastly, the conclusions are discussed.

2 Theoretical Analysis of Planar Coil Calculations

Coil design is a critical factor in maximizing power transfer efficiency in wireless power transfer (WPT) systems. The efficiency of energy transfer is predominantly governed by the mutual inductance between coils, which directly impacts current distribution and overall system performance. Since mutual inductance is a key determinant of coupling efficiency, optimizing coil geometry, spatial configuration, and alignment is essential for enhancing energy transfer capabilities. A well-designed coil not only improves system efficiency but also ensures reliable and stable operation in WPT applications.

2.1 Design Considerations for Coil Parameters

Oversimplified approaches, such relying exclusively on frequency-based tables for selecting strand diameters, can result in suboptimal performance and. certain instances, may even counterproductive. These methods can lead to higher resistance compared to solid wire or foil windings, increasing both energy losses and overall costsproblems that could be mitigated through a more refined and optimized design approach. The proposed methodology is tailored for efficient implementation using spreadsheet software, and its streamlined nature allows for manual calculations, making it versatile and suitable for use in a variety of computational environments. The skin depth (δ) is computed using Equation (1), whereas the maximum recommended number of strands to be braided during the initial stage (N_{1max}) is determined by Equation (2). Here, ρ represents the resistivity of the conductor $(1.72 \times 10^{-8} \,\Omega \cdot m)$ for copper at room temperature, or $2 \times 10^{-8} \Omega \cdot m$ at $60 \circ C$), f denotes the frequency of the sinusoidal current in the winding, Ds is the strand diameter, and μ_0 is the permeability of free space $(4 \times 10^{-7} \pi \frac{H}{m})$. For optimal operation, a current density of $J_{cu} = 4 \frac{A}{mm^2}$ is assumed. The strand count and the diameter of the Litz wire are derived from Equation (3) and (4), respectively. The parameters D_s , A_s , and N_s represent the diameter, cross-sectional area, and number of strands in the Litz wire, respectively. A_{cu} denotes the required cross-sectional area of the wire, which is calculated based on the specified current density. D_{Lcu} Indicates the equivalent diameter of the Litz wire bundle, excluding the insulation. The parameter values for the Litz wire, operating at a frequency of 85 kHz, are summarized in Table 1.

$$\delta = \sqrt{\frac{\rho}{\pi f \mu_0}} \tag{1}$$

$$N_{1,max} = 4 \frac{\delta^2}{Ds^2} \tag{2}$$

$$N_{\rm s} = \frac{A_{cu}}{A_{\rm s}} \tag{3}$$

$$D_{Lcu} = 1.3\sqrt{N_s} \times D_s \tag{4}$$

Table 1. Parameter Values for Litz Wire.

Parameter	f (kHz)	δ (mm)	N _{1max}	N_s	N_{e}	D _{Lcu} (mm)
Value	100	0.2	16	880	55	3.860

The diameter of an individual Litz wire strand is 0.1 mm. Taking into account the insulation between layers and the equivalent diameter of the Litz wire (D_{Lw}) , a diameter of 5.461 mm is chosen for each winding turn to ensure adequate insulation and optimal performance under the specified operating conditions. The values of D_{Lw} and N_e , the effective number of strands, for the designed Litz wire are shown in Fig. 1. N_e is calculated using Equation (5).

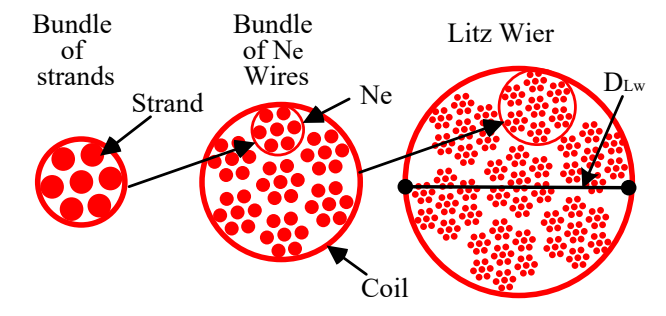


Fig 1. Steps to Litz Wire Manufacturing.

2.2 Ferrite Bars and Aluminum Shielding

Amorphous cores exhibit a higher saturation flux density, typically exceeding 1.5 T, and possess good

thermal conductivity. In contrast, ferrites, despite having a lower saturation flux density (generally below 0.5 T), are favored in electric vehicle WPT systems. This preference stems from their significantly lower magnetic losses and high permeability within the megahertz frequency range. Ferrite materials exhibit high electrical resistivity, effectively mitigating energy dissipation and enhancing overall system efficiency. The incorporation of ferrite cores strengthens the magnetic field, thereby improving power transfer performance. These materials are characterized by wide operational temperature ranges, ensuring stable functionality even under hightemperature conditions. Additionally, ferrite cores are lightweight and can be readily fabricated into diverse geometries, facilitating the structural design and integration of WPT systems. Their inherent electrical insulation properties further contribute to preventing unintended short circuits. To streamline the design process, a standard Type I ferrite core ($40 \times 12 \times 8$ mm) is utilized without alterations or modifications. The dimensions of the selected ferrite core are depicted in Fig. 2. During the wireless charging process of an electric vehicle battery, a high-frequency magnetic field is established between the transmitting and receiving coils. Ensuring that the magnetic flux density remains within established safety limits is critical, particularly when individuals are positioned in standard locations, such as standing near the system. At WPT operating frequencies, regulatory guidelines specify that the permissible magnetic flux density for the general public typically falls within the range of 6.25 μT to 27 μT . To enhance user safety and mitigate electromagnetic interference, an aluminum shielding layer is employed. Fig. 3 presents the simulated distribution of magnetic flux density across a circular pad structure. The implementation of the aluminum shield results in a measured flux density of 13 µT within the protected region, ensuring that vehicle occupants and surrounding electronic equipment situated above the shielded zone are not exposed to hazardous magnetic field levels.

$$k = \frac{M}{\sqrt{L_{Tx}L_{Rx}}} \tag{6}$$

$$Q = \frac{\omega l}{R} \tag{7}$$



Fig 2. Dimensions of the Type I ferrite core (L = length, W = width, and t = thickness).

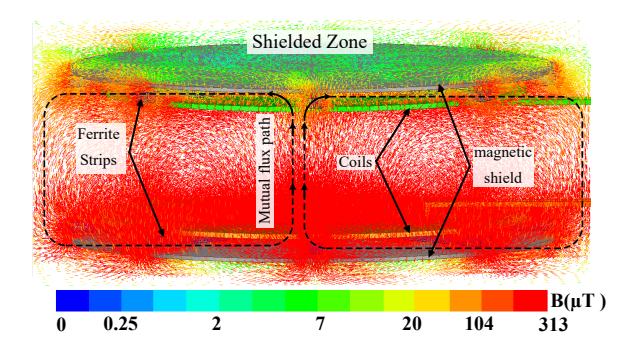


Fig 3. Simulated flux density distribution in a circular pad structure.

3 Topology Design and Performance Comparison

3.1 Design and Simulation

A key technical challenge involves maximizing the coupling coefficient whereas concurrently reducing magnetic flux leakage. Furthermore, the ability to tolerate misalignment is a crucial factor in the design of wireless charging systems for electric vehicles. Maintaining efficient energy transfer despite possible misalignment between the transmitter and the receiver in electric vehicle charging systems is essential for ensuring both reliability and operational efficiency. As a result, the coupling coefficient serves as a key parameter for evaluating and comparing the efficiency and performance of various topologies. As presented in Table 2, it is crucial to establish a range of parameters during the design phase, such as coil length (L_C), coil width (W_C), the quantity of ferrite strings (N_{fs}), the number of bars per string (N_{fb}), the distance between ferrite strings (D_{fs}), coil side dimensions (C_d), pad length (L_p), and pad width (W_p). The coil dimensions are determined by the number of turns (N) and the pitch, which represents the spacing between consecutive turns. Since the DDO configuration offers a more holistic approach, the principal design parameters for a DDQ pad are depicted in Fig. 4. It is important to mention that d, dd, and q, as outlined in Table 2, refer to the respective coil sides. The optimization parameters are summarized in Table 2, while the designed topologies are shown in Fig. 5. FEA is utilized for the simulation process.

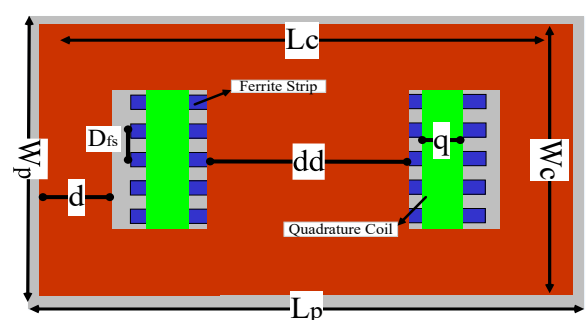


Fig 4. Key design variables of the DDQ pad structure.

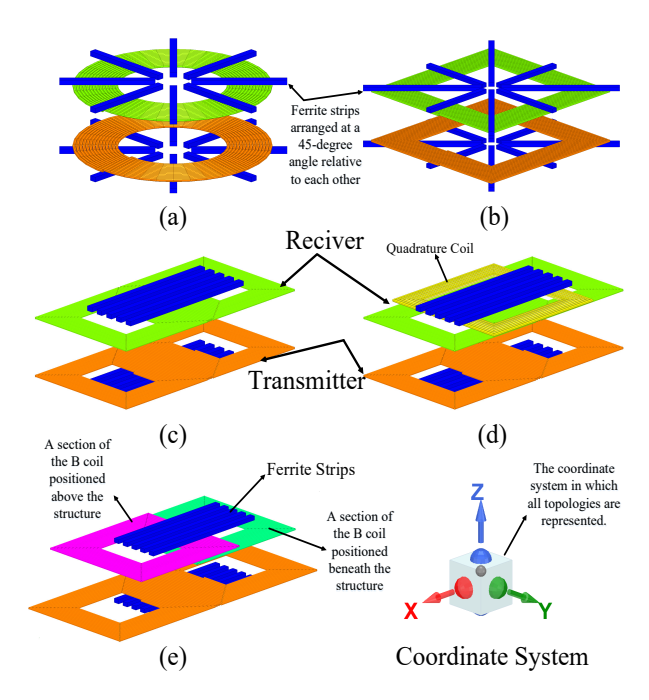


Fig 5. (a) Circle, (b) Square, (c) Double-D (DD), (d) Double-D Quadrature (DDQ), and (e) Bipolar (BP) pad topologies for electric vehicle charging. The coordinate system also indicates the analytical orientation of the X, Y, and Z axes.

Fig. 6 presents a comparison of the coupling coefficients for five distinct topologies at a 100 mm gap, accounting for both lateral and rotational misalignments between the pads. As shown in Fig. 6 (a) and (b), the circular coil accommodates misalignments of up to 13% of the pad diameter in both the X and Y axes. In square coil exhibits comparable contrast, the performance, although slightly less efficient. The DD, DDQ, and BP coils demonstrate enhanced performance along the X-axis compared to the Y-axis. The analysis reveals that the DD, DDQ, and BP coils outperform the circular and square coils in both directions. Specifically, as depicted in Fig. 6(a), the DDQ and BP topologies exhibit superior performance along the X-axis, with a misalignment tolerance of up to 30% of the pad length, which is considerably higher than the 20% tolerance observed for the DD topology.

Fig. 6 (c) depicts the effect of rotational misalignment around the Z-axis. The results indicate that both the circular and square coils maintain stable performance under angular misalignment, with a consistent coupling coefficient observed throughout the entire range of angles. The stable coupling coefficient observed in both square and circular pads during rotational misalignment can be primarily attributed to their structural configuration, which allows them to sustain performance similar to that of an ideal aligned state across the entire angular range. Another factor that contributes to the stability of the coupling coefficient (k) during rotation of

the secondary pad is the analogous variations in both mutual and self-inductance. Consequently, the governing

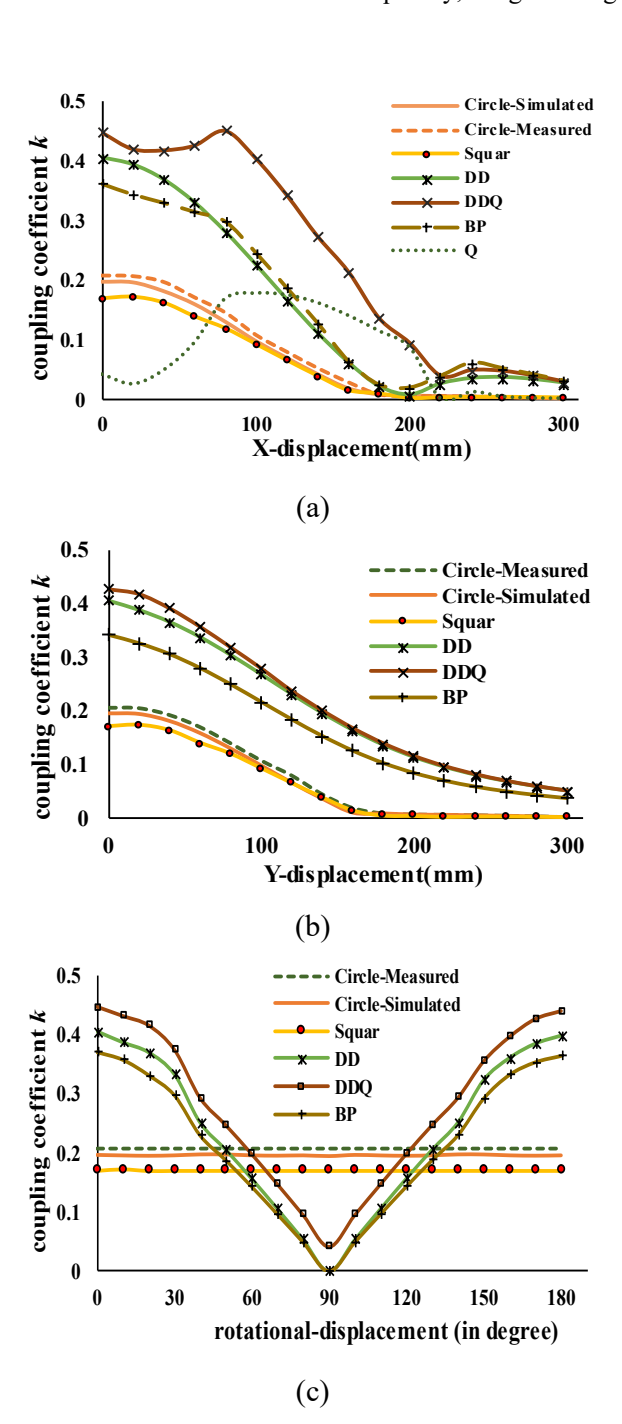


Fig 6. Comparison of the coupling coefficient (k) at a 100 mm gap under lateral and rotational misalignment between pads. (a) x-displacement, (b) y-displacement, and (c) rotational displacement around the z-axis.

Equation (6) for coupling coefficient ensures that its value remains unchanged. In contrast, the DD, DDQ, and BP coil configurations demonstrate efficient

magnetic coupling even with angular misalignments around the Z-axis, maintaining stable performance up to an angle of 30 degrees. However, once this threshold is surpassed, a marked decrease in coupling efficiency becomes evident. The robustness of the coupling coefficient up to 30 degrees of angular misalignment in the DD, DDQ, and BP topologies is attributed to the transmitter pad staying within the permissible horizontal displacement limits. In D-family topologies, when the misalignment angle exceeds 30 degrees, both inductance (L) and mutual inductance (M) decrease. However, the decrease in mutual inductance (M) due to angular misalignment is much more pronounced. Consequently, the coupling coefficient (k) undergoes a significant reduction.

Table2. Optimized Design Parameters for Evaluated Topologies

Parameter	Square	Circular	DD	DDQ	РВ		
L _C (mm)	250	380	419	419	410		
W _C (mm)	250	380	227	227	227		
N	14	14	14	Q D 7 14	14		
N _{fs}	8	8	5	5	5		
N _{fb}	4 & 5	4	7	7	7		
D _{fs}	45(deg)	45(deg)	24(mm)	24(mm)	24(mm)		
C _d (mm)	77	77	d dd 77 152	d dd q 77 152 38	77		
L _p (mm	390	390	430	430	420		
W _p (mm)	390	390	240	240	240		

3.2 Comparative Analysis

As depicted in Figs. 5(a) and 6(b), both the circular and square topologies are composed of two identical coils, with ferrite materials positioned at a 45-degree angle relative to each other. In contrast, the DD structure shown in Fig. 5(c) employs two D-shaped coils for both the transmitter and receiver pads, resulting in a total of four D-shaped coils across both pads. The DDQ topology, illustrated in Fig. 5(d), integrates a DD transmitter coil with a receiver coil that includes two D-shaped coils in addition to a rectangular coil. Lastly, the BP topology, presented in Fig. 5(e), consists of a DD transmitter coil and a receiver coil comprising two identical rectangular coils placed at an optimal distance from one another, with one coil positioned on top and the other beneath.

In designing the control and compensation circuits for circular and square coil configurations, it is assumed that two distinct circuits are required: one to power the transmitter pad and another to capture the energy in the secondary coil. In contrast, for the DD and BP coil configurations, the design of control and compensation circuits must account for four coils, while the DDQ configuration necessitates circuits to support five coils. The higher number of circuits introduces additional complexity to the control system, leading to more sophisticated structural designs. The analysis performed leads to a comparison of commonly used coil pad designs, highlighting their key characteristics such as mutual inductance (M), coupling coefficient (k), number of Litz wire strands and I-cores, surface area, as well as horizontal and rotational misalignments. The complexity of the methods is also considered, and the summarized results are presented in Table 4.

The CP topology, while demonstrating moderate power transfer efficiency, is characterized by a relatively large pad design. Additionally, it presents challenges in terms of manufacturing complexity, construction costs, and control system requirements. The CP topology utilizes fewer materials; however, it is associated with a reduced transmission range and a more confined charging area. Moreover, the control strategies and fabrication processes for this topology are less complex and more economical when compared to other alternative designs. The SP configuration demonstrates performance comparable to the CP structure. However, it incurs a slightly higher manufacturing cost and complexity in comparison to the circular coil design. The DDQ configuration provides enhanced power transfer efficiency and a size comparable to the DD configuration. However, it features a larger charging area than the DD configuration. Despite these advantages, the DDQ structure is associated with higher construction costs, increased material consumption, and a more complex control approach in comparison to the other topologies discussed in this study. The BP coil exhibits characteristics akin to the DDQ coil but provides benefits such as lower manufacturing costs, reduced material requirements, and a straightforward control approach compared to the DDQ configuration. Typically, both BP and DDQ coils are utilized as secondary elements within wireless power transfer (WPT) systems.

4 Assessment of Design Analysis Accuracy

Drawing from the analytical findings in Section 3, the circular coil configuration is recognized as the most straightforward and economically efficient choice for construction. To verify the precision of the finite element analysis (FEA), a circular coil was constructed based on the specifications provided in Section 2. The constructed circular transmitter and receiver pad assemblies, along with a depiction of the simulation model, are presented in Fig. 7. A total of sixteen strands, each 0.1 mm in diameter, were twisted to form a single bundle of Ne. Subsequently, eleven of these bundles

were twisted together to create one coil. To complete the Litz wire configuration, five of these coils were then combined. A 160 mm ferrite core was constructed by combining four separate ferrite cores. According to the optimization results, eight ferrite cores were positioned 30 mm from the center of the pad. The data in Fig. 6(a, c) exhibit a strong agreement between the simulated and measured results, confirming that the simulation model effectively mirrors the physical system. This alignment serves to validate the design and analytical methods applied in this study. Additionally, the self-inductance of the transmitter pad was measured independently using an RLC meter. As depicted in Fig. 8, the measured selfinductance value is $73.97 \mu H$, which is in close agreement with the simulated value of 72.623 µH. This strong correlation validates the accuracy of the fabrication process and reinforces the reliability of the simulation model. The strong alignment between the experimental and simulated results highlights the efficacy of the design approach and confirms that the simulation model accurately represents the actual system behavior. This consistency not only bolsters the reliability of the modeling methodology but also reinforces confidence in the scalability and real-world applicability of the design.

Table3. L and R Characteristics of Coil Topologies

Item	Square	Circular	DD	DDQ	PB	DDZ-DDQZ
L(µH)	84.5	72.26	133	141.6	121.58	162.42
$R(m\Omega)$	14.10	13.74	21.10	23.22	19.31	14.95

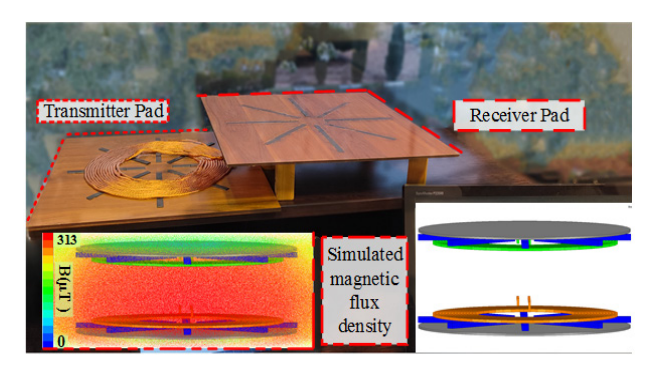


Fig 7. Fabricated circular pad structure and corresponding simulation.

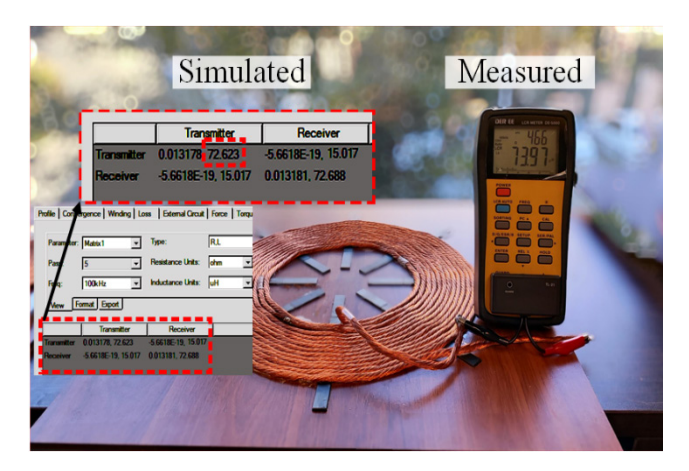


Fig 8. Self-inductance measurement for prototyped circular pad comparing 3D simulation results.

Table 4. Comparison of Different Coil Topologies

Item	Square	Circular	DD	DDQ	PB	unit
K (centered at 100 mm)	0.17	0.196	0.4	0.41	0.34	
M (centered at 100 mm)	14.33	15	52.5	58	47	μН
Litz Wire (T_x+R_x)	28	23	36	39	36	m
I -cores (T_x+R_x)	72	64	70	70	70	Number
Surface area	0.1300	0.1521	0.1032	0.1032	0.1008	m^2
Horizontal Offset	12%x + 12%y	13%x + 13%y	20%x+17%y	29%x+19%y	25%x+17%y	Percentage
Rotational Offset	0-180	0-180	0-28	0-30	0-27	Degree
construction cost	Medium	Low	High	Extremely high	high	

5 Finite Element Analysis of DDZ and DDQZ Planar Coil Architectures

According to the findings presented in Section 3, the DDQ and BP configurations demonstrate superior performance and are identified as the most effective among the five evaluated structures. However, these configurations exhibit limited performance under

angular misalignment. Subsequent research has proposed various advanced coil configurations, including SDD, QDQ, TTP, DDC, Crossed-D, and Zig-Zag, each exhibiting enhanced performance compared to the fundamental structures [11]. However, each of these topologies optimizes only specific aspects of the system and lacks the capability to achieve comprehensive

performance enhancement across all misalignment directions simultaneously. Fig. 9 illustrates the distinct misalignment directions in WPT systems, where Figs. 9 (a), (b) and (c) depict horizontal displacements, Fig. 9(d) represents vertical displacement, and Figs. 9 (e) and (f) correspond to angular misalignments. Building upon the design methodology presented in Section 3 and its validation in Section 4, a novel structure is proposed, exhibiting robust performance across all displacement scenarios illustrated in Fig. 9.

Figure 10 illustrates the simulated representation of the proposed structure. This design is characterized by a novel ferrite arrangement, and due to the resemblance of the transmitter coil to the DD configuration, it is designated as DDZ. Likewise, the receiver coil is referred to as DDQZ. In this configuration, an 810stranded Litz wire with a strand diameter of 0.1 mm is utilized for simulation analyses. Each D coil comprises ten turns, and the combined area of the transmitter (DDZ) and receiver (DDQZ) pads, inclusive of the aluminum shielding, is 0.098 m². To augment magnetic coupling performance, I-shaped ferrite cores with dimensions of 100×30×8 have been incorporated into the design. Through comprehensive dimensional analysis and the optimized arrangement of ferrite cores using Ansys Maxwell, the proposed configuration, as depicted in Fig. 10, achieved the maximum coupling coefficient. Based on the analyses presented in Section 3, the key design parameters—namely, the inter-turn spacing, number of turns, overall dimensions, and air gap—were rigorously established.

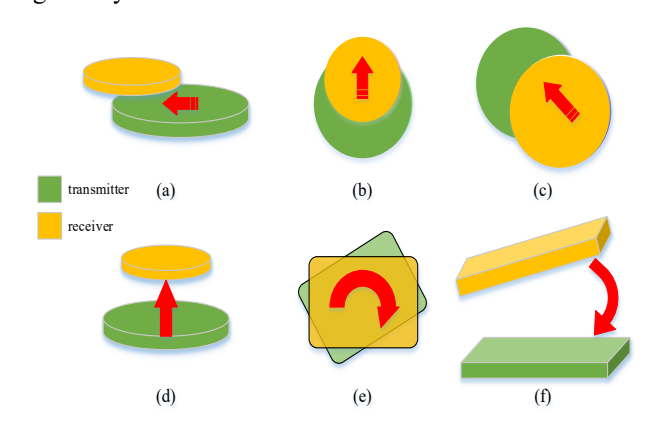


Fig 9. Illustrations of various coil misalignment types: (a) axial, (b) transverse, (c) planar displacement in the XY-plane, (d) height variation, (e) rotational shift, and (f) tilt misalignment [12].

This structure is designed to resemble both a DD configuration and a square shape. The geometric and magnetic parameters are meticulously optimized to ensure that when two D-shaped coils are positioned adjacently, they form a square DD configuration with precise dimensions of 300×300 mm. This magnetic

structure effectively guides the flux along the y-axis, resulting in superior misalignment tolerance. However, along the x-axis, the system can accommodate misalignments of up to 31%, beyond which a null point emerges. To address this limitation, the strategic integration of a square Q coil, as illustrated in Fig. 10, significantly enhances the misalignment tolerance along the x-axis, thereby improving overall system robustness and magnetic performance. As depicted in Fig. 11 (a) and (b), the proposed structure improves performance and exhibits a misalignment tolerance of 44% along the x-axis and 40% along the y-axis. Due to its square geometry, the proposed topology exhibits nearly identical performance along both the x and y axes, furthermore, the overall performance has been significantly enhanced. This confirms that the DDZ-**DDOZ** structure inherits the advantageous characteristics of the SDD configuration. The incorporation of the Q coil further enhances performance along the x-axis, a characteristic similarly exhibited by the DDQ structure.

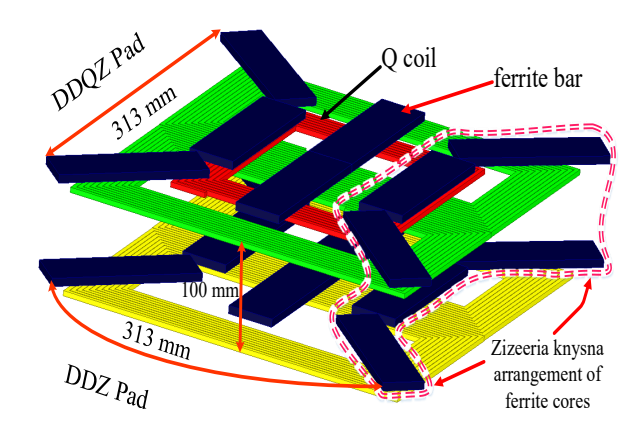


Fig 10. DDZ-DDQZ structure

As illustrated in Fig. 11 (c), under yaw misalignment, the structure maintains stable performance up to 30 degrees and retains acceptable performance up to 45 degrees. This demonstrates that the DDZ-DDQZ structure incorporates the advantageous characteristics SDD, TTP, and DDQ configurations. the Furthermore, unlike the TTP configuration, which necessitates three independent inverters, the DDZ-DDOZ design simplifies the system by eliminating this requirement. Consequently, this structure not only performance improves but also minimizes and manufacturing costs system complexity. Additionally, as presented in Table 3, which outlines the inductance (L) and resistance (R) characteristics of various coil topologies, this configuration effectively decreases winding resistance while increasing selfinductance. According to Equation (7), these improvements lead to a higher quality factor (Q) and enhanced overall system efficiency.

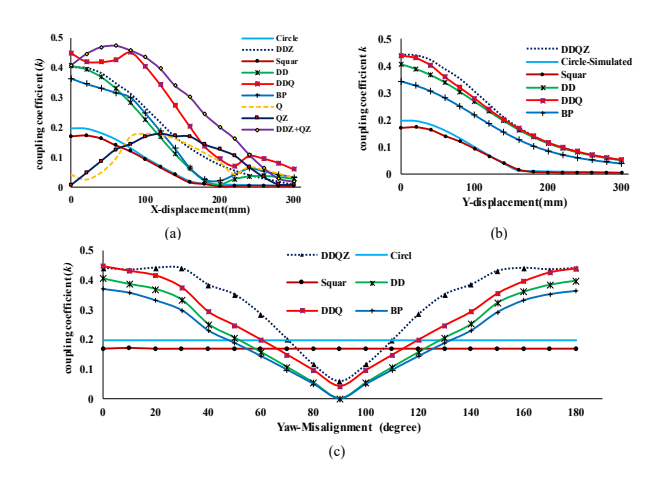


Fig 11. Comparison of the coupling coefficient (k) at a 100 mm gap under lateral and rotational misalignment between pads. (a) x-displacement, (b) y-displacement, and (c) Yaw misalignment.

6 Conclusion

This paper first presents a systematic approach for determining the optimal dimensions of Litz wire and for finite element ferrite cores simulations. Subsequently, five widely used structures in electric vehicle wireless chargers are optimized through finite element analysis. Finally, a fair-performance design framework is established to ensure a balanced and practical evaluation of the optimized structures. The performance of these topologies is compared, and a rigorous evaluation of their respective advantages and limitations is presented. The comparative analysis reveals that, for structures employed in electric vehicle applications, the enhancements in control system and compensation network complexity, manufacturing challenges, and fabrication costs follow the order: DDO > BP > DD > Square > Circle. Based on the conducted analyses, it was determined that the circular topology incurs the lowest cost among all evaluated structures. Consequently, to validate these findings, a circular structure was fabricated and its experimental outcomes were compared with the simulation results. This comparative analysis demonstrated that the finite element analysis method, combined with the design approach for determining the dimensions of Litz wire and ferrite cores, exhibits exceptional accuracy and reliability. Accordingly, using the proposed analysis method, a novel structure was developed that incorporates the advantageous attributes of all preceding configurations while concurrently enhancing system efficiency by optimizing performance in horizontal, vertical, and angular dimensions. This topology exhibits a horizontal misalignment tolerance of up to 44% along the x-axis and 40% along the y-axis. Its performance remains stable with no degradation for yaw misalignments of up to 30°, while the pad can accommodate misalignment angles of up to 45°. Due to its resemblance to the DD topology and its distinctive ferrite core arrangement, this configuration has been designated as DDZ-DDQZ. This novel magnetic structure simultaneously integrates the positive features of the SDD, DDQ, and Tripolar pad configurations, effectively combining their benefits into a single design.

References

- [1] N. Z. Saadabad, Q. Wang and A. Chandra., "Performance Comparison of Coil Geometries in Self-Resonant Wireless Power Transfer System," IEEE Transactions on Industry Applications, pp. 1-9, 2025.
- [2] Z. Zhang, Y. Zhong and X. Mou, "Theoretical Analysis of Litz-Wire DD Coil for Wireless Power Transfer System," 2024 IEEE Wireless Power Technology Conference and Expo (WPTCE), Kyoto, Japan, pp. 646-650, 2024.
- [3] Y. Zhong, Z. Zhang and X. Mou, "Design and Analysis Study of Magnetic Leakage Prevention Based on DD Coil," 2024 IEEE 7th International Electrical and Energy Conference (CIEEC), Harbin, China, pp. 708-712, 2024.
- [4] M. E. Bima, I. Bhattacharya, W. O. Adepoju and T. Banik, "Effect of Coil Parameters on Layered DD Coil for Efficient Wireless Power Transfer," in IEEE Letters on Electromagnetic Compatibility Practice and Applications, vol. 3, no. 2, pp. 56-60, 2021.
- [5] M. Wu et al., "Modeling of Litz-Wire DD Coil With Ferrite Core for Wireless Power Transfer System," in IEEE Transactions on Power Electronics, vol. 38, no. 5, pp. 6653-6669, 2023.
- [6] Y. Liu, R. Mai, D. Liu, Y. Li and Z. He, "Efficiency Optimization for Wireless Dynamic Charging System With Overlapped DD Coil Arrays," in IEEE Transactions on Power Electronics, vol. 33, no. 4, pp. 2832-2846, 2018.
- [7] G. Yang et al., "Interoperability Improvement for Rectangular Pad and DD Pad of Wireless Electric Vehicle Charging System Based on Adaptive Position Adjustment," in IEEE Transactions on Industry Applications, vol. 57, no. 3, pp. 2613-2624, 2021.
- [8] M. E. Bima, I. Bhattacharya, and C. W. V. Neste, "Experimental evaluation of layered DD coil structure in a wireless power transfer system," IEEE Transactions on Electromagnetic Compatibility, vol. 62,no. 4, pp. 1477–1484, 2020.

- [9] G. Wei, X. Jin, C. Wang, J. Feng, C. Zhu and M. I. Matveevich, "An Automatic Coil Design Method With Modified AC Resistance Evaluation for Achieving Maximum Coil—Coil Efficiency in WPT Systems," in IEEE Transactions on Power Electronics, vol. 35, no. 6, pp. 6114-6126, 2020.
- [10] M. Negintaji, A. Ghaheri and E. Afjei, "Optimization and Comparative Study of Wireless Power Transfer Topologies for Electric Vehicles," 2024 4th International Conference on Electrical Machines and Drives (ICEMD), Tehran, Iran, Islamic Republic of, pp. 1-6, 2024.
- [11] M. Behnamfar, T. O. Olowu, M. Tariq and A. Sarwat, "Comprehensive Review on Power Pulsation in Dynamic Wireless Charging of Electric Vehicles," in IEEE Access, vol. 12, pp. 66858-66882, 2024.
- [12] A. Sagar, A. Kashyap, M. A. Nasab, S. Padmanaban, M. Bertoluzzo, A. Kumar, and F. Blaabjerg., "A Comprehensive Review of the Recent Development of Wireless Power Transfer Technologies for Electric Vehicle Charging Systems," in IEEE Access, vol. 11, pp. 83703-83751, 2023.

Biographies



Mohammad Negintaji received his M.Sc. degree in Power Electronics and Electrical Machinery from Shahid Beheshti University, Tehran, Iran, in 2019. He is currently pursuing a Ph.D. degree in Electrical Engineering at Shahid

Beheshti University. His research focuses on the design and optimization of magnetic structures for wireless power transfer systems, with a particular emphasis on wireless charging applications for electric vehicles.



Aghil Ghaheri received his M.Sc. degree in Power Electronics and Electrical Machinery in 2016 and his Ph.D. degree in Electrical Machinery in 2022, both from Shahid Beheshti University in Tehran, Iran. From 2022 to 2024, he worked as a Postdoctoral Researcher in the Department of Electrical Engineering

at Shahid Beheshti University. In 2024, he became an Assistant Professor in the same department. His research interests include electromagnetic, thermal, and structural modeling, as well as the optimization and manufacturing of electrical machines for industrial and renewable energy applications.



Seyed Ebrahim Afjei received the B.S. and M.S. degrees in electrical engineering from The University of Texas at Austin, Austin, TX, USA, in 1984 and 1986, respectively, and the Ph.D. degree in electrical engineering from New Mexico State University, Las Cruces, NM, USA, in 1991.He is currently a

Professor with the Department of Electrical Engineering, Shahid Beheshti University, Tehran, Iran. His current research interests include switched reluctance motor drives and power electronics.